P107598

A STUDY ON THE INTENSITY CHANGE OF TYPHOON NAKRI(0208) -OBSERVATION AND GDAPS DATA ANALYSIS

Baek-Jo Kim*, KiRyong Kang, Chun-Ho Cho, and Hyo-Sang Chung
Meteorological Research Institute, Korea Meteorological Administration

Abstract

Typhoon Nakri(0208), formed as a Tropical Storm (TS) at about 400km southwest of Taiwan on 1800UTC 8 July, 2002, was studied using two Aerosondes and the GDAPS (Global Data Analysis and Prediction System) analysis data.

The evolution of 200-850 hPa vertical wind shear and 200 hPa eddy relative angular momentum flux convergence (EFC) based on the GDAPS analysis data showed that typhoon Nakri has experienced an intensity change since 0000UTC 13 July when the vertical shear exceeds 10 m s^{-1}. It was also found that during the period of interacting with the trough, positive values of EFC was larger than other times. The Aerosonde observations showed that a strong inversion layer and isohume layers exist in the lower tropospheric vertical structures over the ocean ahead of typhoon. Isohume layers are composed of very wet (nearly saturated) below 850 hPa, and dry above 830 hPa during the rapidly weakening period of typhoon.

When the northwesterlies were present at altitude between 1.5km and 3.5km about 3 hours before the typhoon weakened, the trough at 850 hPa moved southward, which was related to a typhoon-trough interaction.

Keywords: Typhoon Nakri, Intensity Change, GDAPS analysis Data, Aerosonde, Typhoon-Trough Interaction.

* Corresponding author address: Baek-Jo Kim, Meteorological Research Institute, 460-18, Shindaebang, Dongjak-gu, Seoul, 156-720, Korea; email: bjkim@metri.re.kr

1. Introduction

Damage to lives and property from severe weathers in summer by typhoon and heavy rainfall in Korea reaches more than 70 percent of annual natural disaster according to the report of National Emergency Management Agency issued in 2002. In particular, heavy rainfall is largely associated with meso-scale convective systems developing along the Changma front (summer rainy season in Korea) and typhoon, which move mainly northward from the East China Sea where few observations are available. The scarcity of observations over the ocean except for the limited use of satellite soundings for initial analyses is believed to limit improvement in the understanding of atmospheric structure of such an meso-scale severe weather systems over the ocean. For better understanding and prediction of severe weather systems, observation data over the ocean are essential.

Many investigators have reported that intensive observations in the environment and core of tropical cyclone would improve the initial representation of tropical cyclones (Burpee et al., 1984; Burpee et al., 1996; Tuleya and Lord, 1997). A few upper-air observations are available in the tropical cyclone environment over the ocean. From this view of point, in Japan, Nakazawa (2001) showed the characteristics of tangential and radial wind speed distributions relative to the typhoon Toraji (0108) center from a series of Aerosonde field campaign. And he pointed out that Aerosonde is one of the appropriate observing systems for tropical cyclone.

In situ measurements using unmanned aircraft and dropwindsondes continue to play a vital role in producing additional observational data over the ocean. The autonomous Aerosonde (Holland et al, 1992) is a small robotic aircraft with a wing-span of 2.9 meters, flight endurance time in excess of 30 h, range exceeding 3,000 km and a ceiling of around 6 km. There is no doubt that the Aerosonde is capable of measuring temperature, humidity, pressure and winds with its standard instrument package. The nature of sounding data from the Aerosonde is radically different from that of traditional radiosondes. However, the Aerosonde generally performed well in comparison with the radiosonde observation except for the observational analysis that the Aerosonde observations are warmer (0.01 1.2℃) and drier (less than 2%) than the radiosonde observations in respective temperature and relative humidity profiles (Soddell et al., 2004). The Aerosonde has covered a wide range of observing region from the Arctic in April 1999 to the south of Japan in June 2005 to obtain meteorological observations (www.aerosonde.com).

The Aerosonde field experiment through the Korea Enhanced Observing Period (KEOP) project, which was initiated in 2001 by the Meteorological Research Institute (METRI), Korea Meteorological Administration (KMA), was conducted over the south ocean off Jeju Island on July 8 19, 2002. Its objective is to understand the atmospheric environmental structure of the environment of typhoon approaching the Korean peninsula from the East China Sea. During this experiment, two different Aerosondes were used to cover the domain within about 200 km south away from Jeju Island on 13 and 14 July, 2002 when typhoon Nakri (0208) experienced a rapid change of typhoon intensity. In this study, we also analyzed the evolution of environmental influences associated with rapid-weakening typhoon from the GDAPS (Global Data Analysis and Prediction System) analysis data.

2. Field Experimental Setup

The Aerosonde observation was made using two different Aerosondes (Serial No. 111: Hargrave, and Serial No. 112: Fysh) developed by the Aerosonde Robotic Aircraft Ltd, Australia in collaboration with Jeju Regional Meteorological Office during the period of 8 to 19 July, 2002. Total flight time of two Aerosondes is 55 hrs 44 min.

Fig. 1 shows the picture of METRI Aerosonde Mark 2 and flight area permitted by the Korea Air Traffic Control Center. This aircraft was developed as a result of an extension program of improvements to increase reliability, robustness, and operational capacity (Holland et al., 2001). It could have 30 hrs' endurance, range of 3000km, and practical altitude ceiling to 5km. Temperature, relative humidity, and pressure is observed by a set of radiosonde instruments tailing in the free airstream, where they are protected from rain and solar radiation by the aircraft wing. Wind data is obtained by a proprietary algorithm using a combination of scalar airspeed from a pivot tube of Aerosonde and vector ground speed from the Global Positioning System (GPS) while Aerosonde performs a partial circle or S-turn maneuver.

The flight area is a temporary limited area off the coast of Jeju Island (South Korea) to the south ocean of Jeju Island. More detailed latitude and longitude points are given in the caption of Fig. 1. The comprehensive meteorological information for determining the optimal flight route and altitude, launching/recovery time of Aerosonde at least 24 hours in advance is essential for the successful flight of Aerosonde. Considering this aspect, Gosan weather station with a good communication facilities, located in the western edge of Jeju Island as given in Fig. 1, is selected as the headquarter of Aerosonde field experiment. The Moseulpo airport lies in the southwestern part of Jeju Island surrounding with a flat farmland except for Mt. Sanbang to the north and oceans to the south and west. It might be thought from this circumstances that this airport is a good place for the Aerosonde launching/recovery site because of the absence of remarkable obstacles. In particular, the low possibility of Aerosonde meeting topographically-induced strong wind when it is flying over Seogwipo city south of Mt. Halla (1,950 m) is another reason to be chosen the Moseulpo airport as the Aerosonde launching/recovery site in the aspects of its safety.

Fig. 2 shows the 3-dimensional flight routes over the Aerosonde Hargrave and Fysh. On 13 and 14 July, two Aerosondes flew about over the south ocean off Jeju Island. Aerosonde Hargrave took off the Moseulpo airport at 0845UTC 13 July and landed there at 0300UTC 14 July. Its flight time is 19 hrs 17 min. On the other hand, Aerosonde Fysh was also launched from the Moseulpo airport at 0550UTC 13 July and came back to the site at 0030UTC 14 July, 2002. Its flight time is 19 hrs 46 min. Aerosonde Hargrave's observing mission is to make soundings at targeting points which are located at about 50 km and 100 km south of the Moseulpo airport (Fig. 2). In case of Aerosonde Fysh with its flight mission of ascending/descending flight at the distance of 170～ 10 km southwest of the Moseulpo Airport, it flied southwestward for about 4 hours with a constant flight altitude of 1.5 km during the ascending flight up to 1.5 km during the initial flight period. Thus, it flew into the altitude between 1.5 km and 2.5 km from 0935UTC to 1530UTC 13 July.

These Aerosondes are forced to make meteorological observations with their gradual ascending and descending flight while they are moving southward to a targeting point. As a result, the flight trajectories of Aerosonde have saw-toothed, as shown in Fig. 7. And the highest altitude of Aerosonde observation becomes higher in proportional to the Aerosonde's horizontal flight distance from its launching site in order to solve effectively the communication problem between an Aerosonde ground system and an flying Aerosonde itself caused by a earth curvature. The increased lowest and decreased highest altitudes in Aerosonde's flight is a necessary requirement for the stable collection of Aerosonde observation data against poor communication with ground communication system caused by earth curvature when it flies further southward.

3. Data and Methods

3.1 Data

Before the analysis of Aerosonde observations associated with rapid-weakening typhoon Nakri(0208), we examined the evolution of environmental influences on typhoon intensity. For this diagnostic analysis, six-hourly gridded data (grid number : 640 in zonal direction and 321 in meridional direction) with horizontal resolution of 0.562° from 0000UTC 10 to 0000UTC 13 July, 2002 are used. The gridded analyses were interpolated bilinearly in the horizontal to tropical cyclone–centered cylindrical grids (41×48) with grid spacings Δr = 50 km and $\Delta \lambda$ = 7.5°.

A 40-hour Aerosonde observation data obtained July 13～ 4 2002 when typhoon Nakri(0208) was slowly moving northward. During the Aerosonde observing period, pressure, temperature, and relative humidity data from each of two meteorological sensors of Vaisala RSS901 carried on board the Aerosonde and wind data from Aerosonde's wind finding manoeuvres are employed in this study. Pressure, temperature and humidity are logged approximately every ten seconds during Aerosonde flight. Wind measurements are logged by each time where the aircraft performs a wind finding manoeuvre. Data-recording frequency is variable and is dependent on flight plan structure.

In addition, synoptic weather charts for two days provided by KMA were used for analyzing the synoptic weather features during the field experiment. TRMM (Tropical Rainfall Measuring Mission) Microwave Imager (TMI) Optimum Interpolation (OI) Sea Surface

Temperature (SST) and AMSR-E data were employed to see an oceanic environmental influences on typhoon intensity.

3.2 Methods

The central pressure of Typhoon Nakri (0208) decreased to 990.0 hPa from 996.0 hPa during a day. Typhoon intensity depends on many environmental factors, including sea surface temperature (SST), upper-tropospheric trough interactions, vertical wind shear, eyewall replacements cycles etc. In this study, 850-200 hPa vertical wind shear and 200 hPa eddy relative angular momentum flux convergence (EFC), which is a measure of typhoon-upper tropospheric trough interaction, are computed by using GDAPS analysis data.

The vertical wind shear is calculated using area-weighted azimuthal mean Cartesian wind components following the methodology of Molinari (1993). The averaging procedure removes a symmetric vortex, so that the winds provide a measure of the environmental flow across the storm. The components of this mean cross-storm wind over the inner 500 km of radius are given by

$$\langle U \rangle = \frac{1}{A} \sum_{i=1}^{5} \left(\frac{\overline{U_{i-1}} + \overline{U_i}}{2} \right) A_i$$
$$\langle V \rangle = \frac{1}{A} \sum_{i=1}^{5} \left(\frac{\overline{V_{i-1}} + \overline{V_i}}{2} \right) A_i$$

where U and V are the cartesian wind components, i is the radial index, indicates an area average, the overbar is an azimuthal average, and A_i represents the areas of 100-km-wide annular rings. The 850–200 hPa vertical shear for each observation time is then calculated from the area-averaged cartesian wind components.

The presence of a trough in the vicinity of a tropical cyclone does not necessarily indicate that an interaction is occurring. There must be a relative approach of the trough and tropical cyclone for favorable dynamical interactions to occur. The EFC acts as a measure of the outflow layer spinup of the tropical cyclone as the trough comes into the volume.

The EFC was defined by Molinari and Vollaro (1990) :

$$EFC = -\frac{1}{r^2} \frac{\partial}{\partial r} r^2 \overline{u'_L v'_L}$$

where u and v are the radial and azimuthal velocity components, respectively; r is the distance from the storm center; the primes indicate the deviation from the azimuthal mean; and the subscript L refers to storm-relative flow. The EFC is calculated at 200 hPa over a radial range of 300–600 for all times in this case.

4. Synoptic Weather Features

Fig. 3 shows the synoptic weather charts at surface and 500 hPa at 1200UTC 12 July, 0000UTC and 1200UTC 13 July, 2002 when two Aerosondes flew about over the south ocean off Jeju Island. Tropical Storm (TS) Nakri(0208) on 1200UTC 12 July has weakened to Tropical Depression (TD) at 1200UTC 13 July during a day on its path toward the south ocean off Jeju Island. It formed as a TS at about 400km southwest of Taiwan on 1800UTC 8 July and has seldom experienced an intensity change with an abnormal track until 0000UTC 13 July. In particular, during 12 and 13 July, this tropical cyclone moved straight northward along the eastern periphery of western North Pacific subtropical high extending to the eastern coastal region of the Kyushu region, Japan and then reached at about 310km south of Jeju Island(Fig. 3a). Strong low-level southwesterly flow whose velocity recorded more than 24 m/s in the western side of the Kyushu region, Japan at 850 hPa was observed after the disappearance of spiral cloud imagery associated with TS (not shown). This means that the large-scale Asian summer monsoon circulation with warm and humid air may affect the Aerosonde-flying domain after tropical cyclone. In 500 hPa, there was a broad trough centered about at the longitude of Korea. A very slow-moving low closed with contour of 5700 gpm was present over the Maritime Provinces (of Siberia) by 1200UTC 13 July when tropical storm Nakri was located over south ocean off Jeju Island (Fig. 3b). At this time, tropical storm Nakri weakened and its northward motion was halted. The synoptic weather features revealed that tropical storm Nakri began to interact with a mid-tropospheric trough at 0000UTC 13 July. Tropical storm Nakri was merging with the 500 hPa trough circulation as it moved into the East China Sea and was changed to TD at 1200UTC 13 July.

Fig. 4 depicts 3-hourly GMS imageries with superimposed sea fog distribution from 0000UTC to 2100UTC 13 July, 2002 obtained from the sea fog detecting algorithm that was developed in KMA for operational use. This algorithm is based on the difference between sea surface temperature and cloud top temperature. It is clearly seen that an inward spiral feature in the cloud disappeared at 1200UTC 13 July. After this time, cloud shield with shape of feathers was predominant to the south of tropical cyclone center. Also it is shown that typhoon Nakri's central pressure sharply increased from 990.0 hPa to 996.0 hPa within a 18 hour period. The location of tropical cyclone center, which is based on the Best Track Data provided by the Joint Typhoon Warning Center (JTWC), remained stationary, particularly in the longitudinal direction. It means that tropical cyclone Nakri, keeping its location nearly fixed, lost its tropical cyclone's property and then was changed to a TD during a day. Based on Fig. 4, it is appeared that the Aerosonde passed just to the north of the typhoon. During a day, sea fog was widely distributed the northwest of Nakri's center with favorable conditions of cold sea surface and inflow of relatively warm and humid northeasterlies associated with typhoon to be shown later. It can be found that the range and intensity of sea fog is closely tied to the intensity of typhoon subjectively judged from the satellite-revealed cloud pattern. In particular, the sea fog-appearing areas were so limited during the period of 1200UTC to 2100UTC 13 July when the northeasterly inflow associated with tropical cyclone was very weak.

It might be anticipated that typhoon Nakri interacted with a 500 hPa trough with its axis of the Korean peninsula at 0000UTC 13 July, indicating that typhoon-upper tropospheric trough interactions may have played an important role in the observed intensity changes. Tropical storm Nakri experienced a rapid change of typhoon intensity, so it abruptly was changed to a TD over the East China Sea.

5. Results

5.1 Environmental influences

It is well known that an environmental wind, which has strong vertical wind shear, disrupts the intensification process and causes typhoon to be weaken (Barrett, 1999). In fact, vertical wind shear is often cited as one of the primary reasons that typhoons do not fully reach their maximum potential intensity. DeMaria et al. (1993) carried out a systematic evaluation of tropical cyclone intensity change using three years of Atlantic storms. They found three major influences: (i) vertical wind shear, (ii) a measure of the amount by which the storm was under its maximum potential intensity (MPI) determined empirically from sea surface temperature (SST), and (iii) a measure of the strength of trough interaction. The last item was evaluated using flux convergence of angular momentum by azimuthal eddies (Pfeffer and Challa 1981 ; Holland and Merrill 1984 ; Molinari and Vollaro 1989) averaged within 600 km of the tropical cyclone center.

Fig. 5 shows the temporal variations of sea level pressure (SLP), 850-200 hPa vertical shear, the EFC computed over the radial range of 300–600 km from 0000UTC to 1200UTC 13 July. The computed SLP was different from the observed central pressure of typhoon, particularly during the period of 1800UTC 10 July to 0000UTC 13 July when the observed central pressure of typhoon showed the constant value of 990hPa, which means that the area-averaged SLP around typhoon is quite different from the central pressure of typhoon (Fig. 5a). However, this SLP has similar trend with the central pressure of typhoon from 0600UTC 13 July. The increasing trend of SLP generally matches with that of 850-200 hPa vertical wind shear. But the magnitude of vertical wind shear has a wide range of 0 to 10 ms^{-1} (Fig. 5b). Zehr (1992) found that tropical cyclones fail to develop when the 850–200 hPa vertical shear is greater than 12.5–15 ms^{-1}. Also he pointed out that the majority of observed weakening periods and periods with no pressure change occur for vertical shear greater than 10 ms^{-1}. According to this threshold value, tropical storm Nakri had experienced an intensity decrease since 0000UTC 13 July when the vertical shear exceeded 10 ms^{-1}. As a result, it was changed to a TD.

At 1800 UTC 12 July, EFC at 200 hPa suddenly increased to about 13 $ms^{-1}day^{-1}$. During the period of 1800UTC 12 July to 0600 UTC 13 July, EFC value was generally higher than in the previous period of 1200 UTC 10 July to 1200 UTC 12 July. DeMaria et al. (1993) used EFC > 10 $m\ s^{-1}\ day^{-1}$ at 200 hPa to indicate a trough interaction. A trough interaction will be said to occur when EFC at 200 hPa exceeds 10 $ms^{-1}day^{-1}$ for at least two consecutive 12-hour periods. According to this criterion, it can be found that typhoon Nakri has interacted with the trough during the period of 1800UTC 12 July to 0600UTC 13 July when positive values of EFC is larger than other times.

In order to examine the possible effect of sea surface temperature on intensity change, daily SST distributions on July 12-13 are given in Fig. 6. It is found that SST less than 24℃ over south ocean off Jeju Island originated from the southern part of Yellow Sea on 12 July were extended southeastward to around the Philippine through the East China Sea. It could be noted that tropical storm Nakri encountered lower SST over the East China Sea on 13 July. Under normal circumstance, we would expect that tropical storm Nakri moving over these waters underwent substantial weakening. In addition, it is deduced that since typhoon Narki remained over lower SST for a long time, the energy loss of the typhoon could be large, too.

5.2 Aerosonde-observed characteristics associated with rapid-weakening typhoon

Fig. 7 shows the time series of altitude and wind (meridional, zonal, and vertical wind speed) observed by Aerosondes. The evolution of wind direction from two Aerosondes showed the transition of southeasterlies to northeasterlies before typhoon weakened, indicating that they were flying from an influencing region of western North Pacific subtropical high to an affecting region of typhoon (Fig. 4). The southeasterlies reflect a divergent flow along the northwestern periphery of the western North Pacific subtropical high. Based on satellite image shown in Fig. 4, Aerosondes were flying within a spiral cloud appearing at the northwest sector of typhoon, implying that they are affected by a convergent flow associated with typhoon. Predominant southwesterlies over Aerosonde-flying region were mainly due to the influence of Asian summer monsoon circulation with southwesterly after typhoon weakened rapidly.

During the period with dominant monsoon flow, wind speed increased suddenly, in particular in case of Aerosonde Fysh, when it was descending up to around 500 m. It is largely contributed by a increased meridional wind with the northward shift of strong low-level southwesterly flow described before. This partly contributed to the fact that mean wind speed of Aerosonde Hargrave is 8.6 m/s, which is somewhat weaker than that of Aerosonde Fysh. The presence of northwesterlies at altitude between 1.5km and 3.5km about 3 hours before typhoon weakened rapidly means the southward movement of trough at 850 hPa, which is related to a typhoon-trough interaction. The ending time of northwesterlies is in good agreement with the beginning time of typhoon-trough interaction obtained from the GDAPS analysis data. In addition, the appearing time of southwesterlies becomes earlier in Aerosonde Fysh than in Aerosonde Hargrave, indicating the gradual northward progression of dominant southwestelies. As a result, low-level circulation features show a mixed monsoon-typhoon flow which is evolved from the flow of typhoon itself.

In order to examine the characteristics of lower tropospheric vertical structure ahead of typhoon along the longitudinal distance away from the Moseulpo airport, the vertical profiles of temperature and relative humidity data observed by two Aerosondes during the whole flight period and each sounding flight period are presented in Figs. 8 and 9. In composited profiles based on Aerosonde data from the left wing sensor of Aerosnde Fysh from 0550 UTC 13 July to 00000 UTC 14 July, the observation data concentrated around 4 levels of 930.0 hPa, 836.5 hPa, 823.0 hPa and 782.0 hPa imply the altitudes of Aerosonde's flight used when it moved horizontally from one targeting point to another one or when it took a short horizontal flight in the ascending/descending flight. First and last, the outstanding feature is the existence of strong lower tropospheric inversion layer in the temperature profile and isohume layers with very wet below 850 hPa and dry above 830 hPa in the relative humidity profile (Fig. 8). The increasing rate of temperature within the inversion layer is 0.068℃ hPa (21.0℃ at 836.0 hPa and 18.8℃ at 868.0 hPa). The inversion layer is partly explained by adiabatic warming caused by subsidence around the western North Pacific subtropical high. The humidity difference between very wet and relatively dry layers is approximately 30 %, indicating that the existence of a nearly saturated layer below 850 hPa associated with the formation of sea fog or stratus clouds and the overlying dry air above 850 hPa with the subsiding air. The sea fog is explained as a result of warm and humid air accompanied by typhoon passing over relatively cool SST. Compared with the temporal variation of wind shown in Fig. 6, strong wind speed was found at approximately the 1.5 km level which is lower than the inversion base.

The inversion base observed by Aerosonde Hargrave becomes higher with the longitudinal distance from the launching site (Fig. 9). That is, it appeared at 918.0 hPa height at 50 km to the southwest from the launching site (in the second ascending flight) and 860.0 hPa height at 135 km (in the third ascending flight). The change of inversion base was small but inversion top was somewhat large with the north-south movement of Aerosonde (Fig. 9). Most ascending flights of Aerosonde Fysh were taken above 850 hPa level except for the first ascending flight which reached up to 850 hPa level. The lapse rate of temperature becomes larger as Aerosonde flies northward to the Moseulpo airport, for example, 0.044℃ hPa at 210 km away from the Moseulpo airport and 0.063℃ hPa at 150 km. In addition, there were inversion layers at 860 hPa level in both the eighth and ninth ascending flights but its intensity was somewhat stronger in the former flight (0.096℃ hPa) than in the latter one (0.091℃ hPa). The vertical profile of relative humidity in Aerosonde Fysh is similar with that of Aerosonde Hargrave. The most interesting thing is that relative humidity tends to decrease as the location of ascending/descending flight becomes northward. This means the intrusion of relatively dry air associated with southeastward moving midlatitude synoptic system into the Aerosonde-flying region after the disappearance of typhoon, affecting the atmospheric vertical structure over the ocean above 850 hPa ahead of typhoon.

5. Summary and concluding remarks

The intensive field-based experiment so called the Korea Enhanced Observing Period (KEOP) has been conducted by the Meteorological Research Institute (METRI), Korea Meteorological Administration (KMA), to produce intensive observation data during the severe weather in summer season, In particular, the Aerosonde observation was made over the southwest ocean off Jeju Island using two different Aerosondes (Serial No. 111: Hargrave, and Serial No. 112: Fysh) developed by the Aerosonde Robotic Aircraft Ltd, Australia in collaboration with Jeju Regional Meteorological Office during the period of 8 to 19 July, 2002. During this field observation, Aerosondes flew about over the domain within about 200 km south away from Jeju Island on 13 and 14 July, 2002 when Tropical Storm (TS) Nakri(0208) at 1200UTC 12 July has weakened to Tropical Depression (TD) at 1200UTC 13 July during a day on its path toward the south ocean off Jeju Island. In this study, we analyzed the evolution of environmental influences associated with rapid-weakening typhoon from the GDAPS analysis data and the characteristics of lower tropospheric vertical structure over the ocean ahead of the weakening typhoon using Aerosonde observation data on 13 and 14 July, 2002.

The synoptic weather features revealed that typhoon Nakri began to interact with a mid-tropospheric trough at 0000UTC 13 July. It is clearly seen from 3-hourly GMS imageries and sea fog distribution that after the interaction of 12 hours, an inward spiral feature in the cloud disappeared and sea fog-appearing areas were so limited.

The evolution of 200-850 hPa vertical wind shear and EFC as environmental influences on typhoon intensity from the GDAPS analysis data showed that typhoon Nakri has experienced an intensity change since 0000UTC 13 July, 2002 when the vertical shear exceeds 10 ms^{-1}. It can also be found that during the period of interacting with the trough, positive values of EFC is larger than other times. In addition, typhoon Nakri encountered lower SST over the East China Sea on 13 July, giving a hint that its moving over these low waters underwent substantial weakening.

Aerosonde observations showed the presence of northwesterlies at altitude between 1.5 km and 3.5 km about 3 hours before typhoon weakened, trough at 850 hPa moved southward, which is related to a typhoon-trough interaction. The ending time of northwesterlies is in good agreement with the beginning time of typhoon-trough interaction obtained from the GDAPS analysis data. Predominant southwesterlies over Aerosonde-flying region after typhoon weakened were mainly due to the influence of Asian summer monsoon circulation.

In addition, one of the Aerosonde -observed characteristics is the existence of strong lower tropospheric inversion layer and isohume layers with very wet below 830 hPa and dry above 850 hPa. The inversion layer is partly explained by adiabatic warming caused by subsidence around the western North Pacific subtropical high. The spatial and temporal behavior of the inversion observed by Aerosonde is dependent on the characteristics of divergence and subsidence associated with the large oceanic western North Pacific subtropical high. The humidity difference between very wet and relatively dry layers is approximately 30 %, indicating that the existence of a nearly saturated layer below 850 hPa associated with the formation of sea fog or stratus clouds and the overlying dry air above 850 hPa with the subsiding air. The Aerosonde-observed characteristics associated with typhoon showed that the spatial and temporal behavior of the inversion is dependent on the characteristics of divergence and subsidence associated with the large oceanic western North Pacific subtropical high. In particular, the inversion base is very much affected by distance from the semi-permanent anticyclonic center. Further finding is that relative humidity tends to decrease as the location of ascending/ descending flight becomes northward, reflecting the intrusion of relatively dry air associated with southeastward-moving mid-latitude synoptic system into the Aerosonde-flying region after the disappearance of typhoon. It might be thought that this kind of lower tropospheric vertical structure features over the ocean ahead of typhoon experiencing an intensity change can be well captured by Aerosonde.

This study provides an observational evidence that lower tropospheric vertical structure features over the ocean ahead of typhoon experiencing an intensity change can be well captured by Aerosonde. Thus, the Aerosonde is thought to be one of the observing systems over the ocean with sparser observation data than over land, which covers a variety of observation data. It also provides a useful observation data for clarifying the atmospheric vertical structure ahead of typhoon approaching from the East China Sea. However, the horizontal and vertical ranges of Aerosonde flight due to unsolved problems of communication link and icing prove still some limitations in the understanding of atmospheric vertical structure over ocean ahead of typhoon. Recently, Kim et al. (2003) identified the central structure of typhoon Rusa (0215) based on 3-hourly upper-air sounding data obtained from Autosonde. It would be mentioned that adpative observations for typhoon based on advanced meteorological equipments together with satellite is required for better understanding typhoon structure approaching the Korean peninsula

Acknowledgements: This study was partly supported by the principal project of METRI "Korea Enhanced Observing Period, KEOP".

References

Barrett, 1999 : *Estimating the amount of rainfall associated with tropical cyclones using satellite techniques*, WMO technical document, NO. TCP-42, pp. 290.

Burpee, R. W., D. G. Marks, and R. T. Merrill, 1984 : An assessment of Omega dropwindsonde data in track forecasts of hurricane Debby (1982). *Bull. Amer. Meteor. Soc.*, **65**, 1050-1058.

Burpee, R. W., J. L. Franklin, S. J. Lord, R. E. Tuleya, and S. M. Aberson, 1996 : The impact of Omega dropwindsondes on operational hurricane track forecast models, *Bull. Amer. Meteor. Soc.*, **77**, 925-933.

DeMaria, M., Baik J.-J., and Kaplan J., 1993: Upper-level eddy angular momentum fluxes and tropical cyclone intensity change. *J. Atmos. Sci.*, **50**, 1133–1147

Holland, G. J., T. McGeer, and H. Youngren, 1992 : Autonomous Aerosondee for economical atmospheric soundings anywhere on the globe. *Bull. Amer. Meteor. Soc.*, 73, 1987-1998.

Holland, G. J., and Merrill R. T., 1984: On the dynamics of tropical cyclone structural changes. *Quart. J. Roy. Meteor. Soc.*, 1**10**, 723–745.

Holland, G. J., and Coauthors,, 2001: The aerosonde robotic aircraft: A new paradigm for environmental observations. *Bull. Amer. Meteor. Soc.*, **82**, 889–902.

Kim, Baek-Jo, Hyo-Sang Chung, Chun-Ho Cho, Jeong-Hoon Kim, 2003 : Structural Features of Typhoon RUSA's Center, *Vaisala News*, 162, 4-7.

Molinari, J., and Vollaro D., 1989: External influences on hurricane intensity. Part I: Outflow layer eddy momentum fluxes. *J. Atmos. Sci.*, **46**, 1093–1105.

Molinari, J., and Vollaro D., 1990: External influences on hurricane intensity. Part II: Vertical structure and response of the hurricane vortex. *J. Atmos. Sci.*, **47**, 1902–1918.

Molinari, J., 1993: Environmental controls on eye wall cycles and intensity change in Hurricane Allen (1980). *Tropical Cyclone Disasters*, J. Lighthill, Z. Zhemin, G. Holland, and K. Emanuel, Eds., Peking University Press, 328–337.

Nakazawa, T., 2001 : Typhoon Hunter 2001 by Aerosonde in Japan, *Proceedings of International Workshop on Observation and Forecasting of Severe Weathers associated with KEOP (IWOF-KEOP), Jeju, Korea, Nov. 13-14, 2001*, 91-94.

Pfeffer, R. L., and Challa M., 1981: A numerical study of the role of eddy fluxes of momentum in the development of Atlantic hurricanes. J. Atmos. Sci., **38**, 2393–2398.

Soddell, J. R., K. McGuffie, G. J. Holland, 2004 :Intercomparison of atmospheric soundings from the Aerosonde and radiosonde, *J. Appl. Meteor.*, **43**, 1260-1269.

Tuleya, R. E. and S. J. Lord, 1997 : The impact of dropwindsonde data on GFDL hurricane model forecasts using global analysis. *Weather and Forecasting*, **12**, 307-323.

Zehr, R. M., 1992: *Tropical cyclogenesis in the western North Pacific.* NOAA Tech. Rep. NESDIS 61, 181 pp.

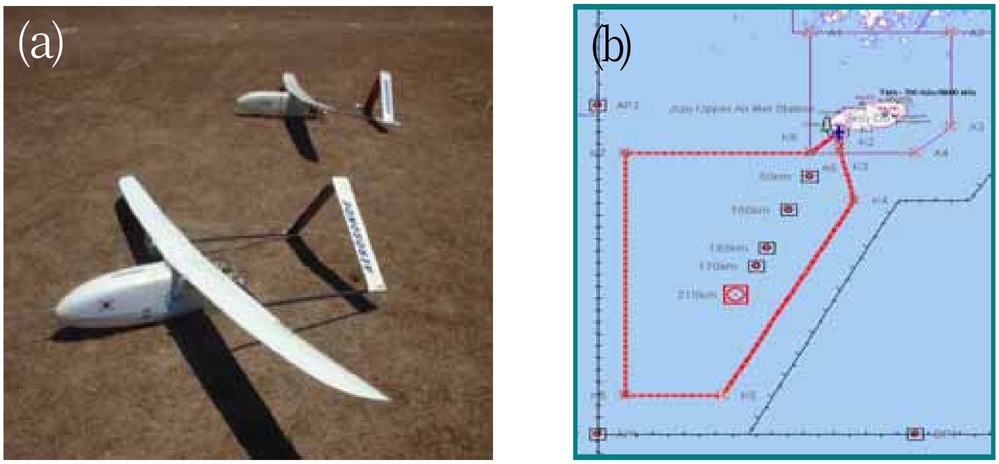

Fig. 1. The picture (a) and flight area (b) of Aerosonde. Airspace is allocated by the local airspace authorities as a temporary limited area off the coast of Jeju Island to the South and South West of Jeju whilst remaining in UHF radio contact. The temporary limited area is bounded by the following points: 33.15N 126.18E - 33.07N 126.17E - 33.00N 126.17E - 32.30N 126.25E - 30.25E 125.10N - 30.25N 124.15E - 33.00N 124.15E - 33.00N 126.00E - 33.15N 12618E.

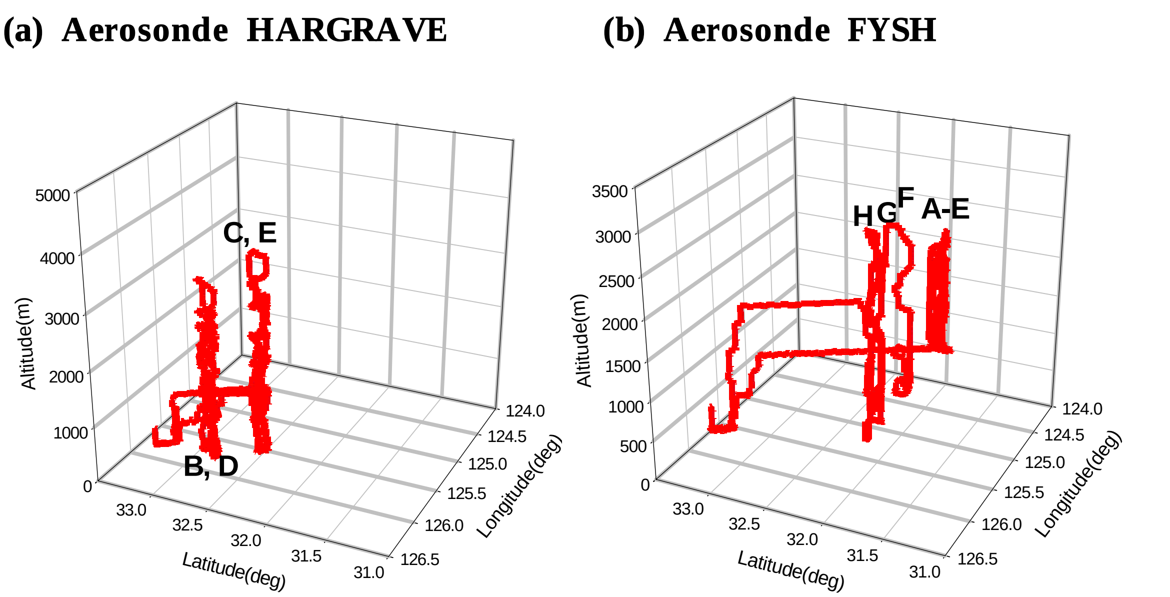

Fig. 2. The 3-dimensional flight routes of (a) Aerosonde Hargrave and (b) Aerosonde Fysh. The alphabet denotes the sequences of ascending/descending flight.

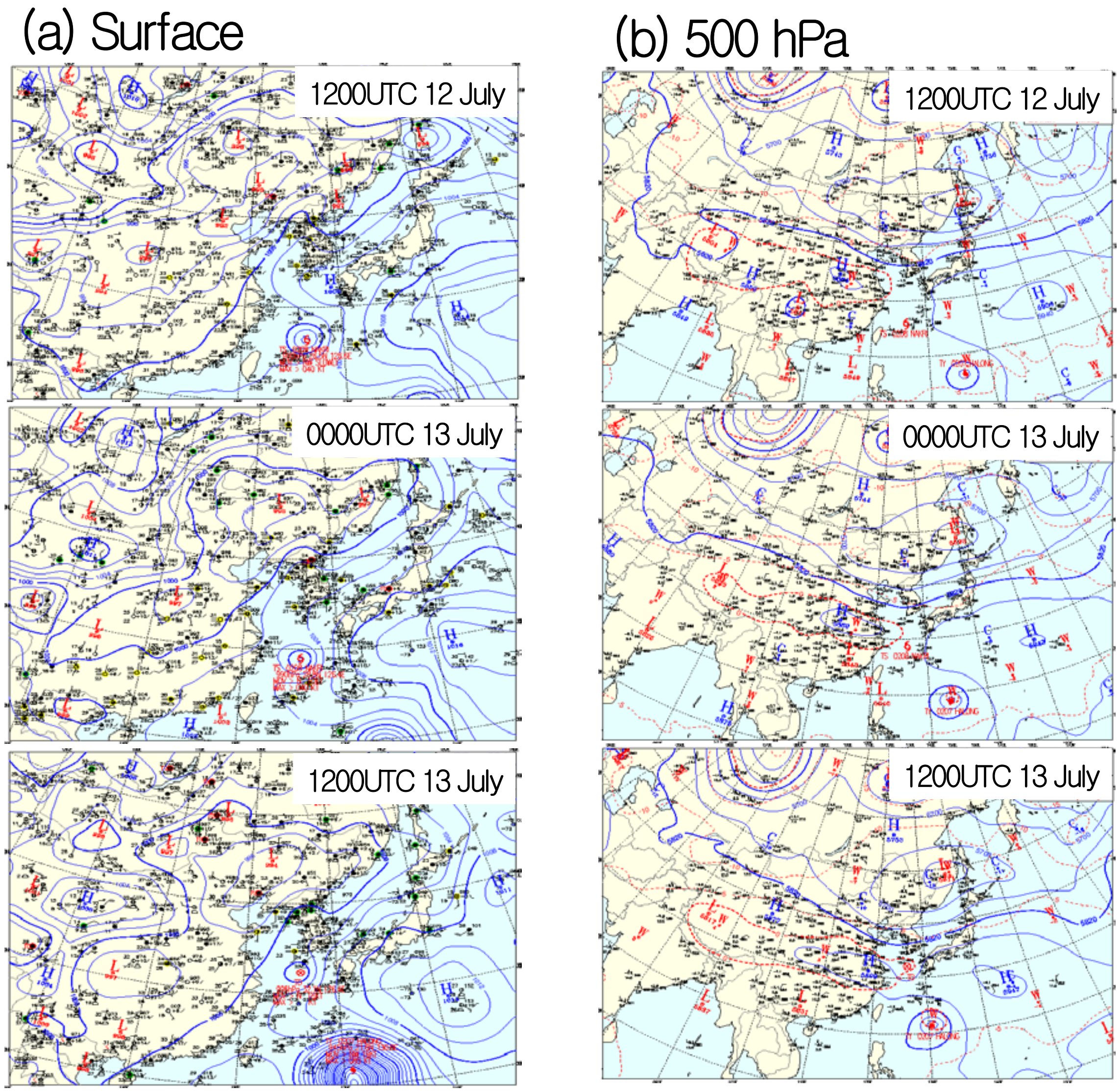

Fig. 3. Synoptic weather charts at surface(a) and 500 hPa(b) at 1200UTC 12 July (upper panel), 0000UTC 13 July (middle panel), and 1200UTC 13 July (bottom panel), 2002.

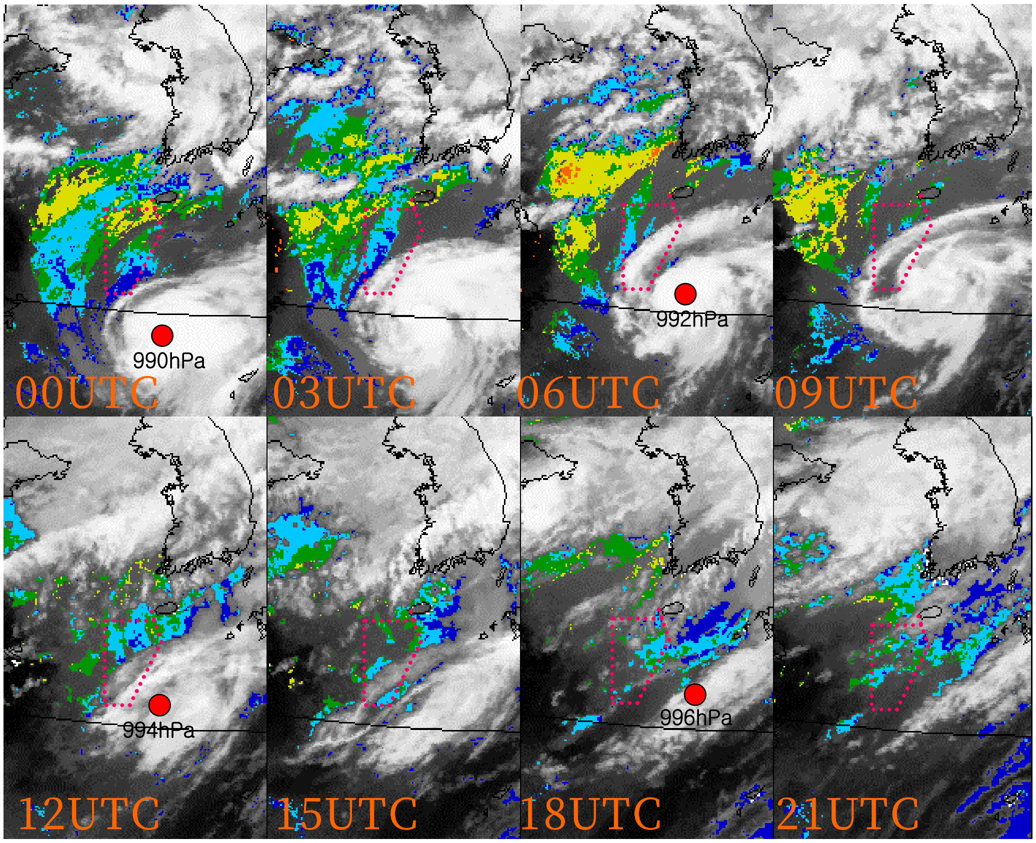

Fig. 4. 3-hourly infrared cloud images and sea fog distributions obtained from GMS satellite data from 0000UTC to 2100UTC 13 July, 2002. An airspace area is enclosed by dotted line.

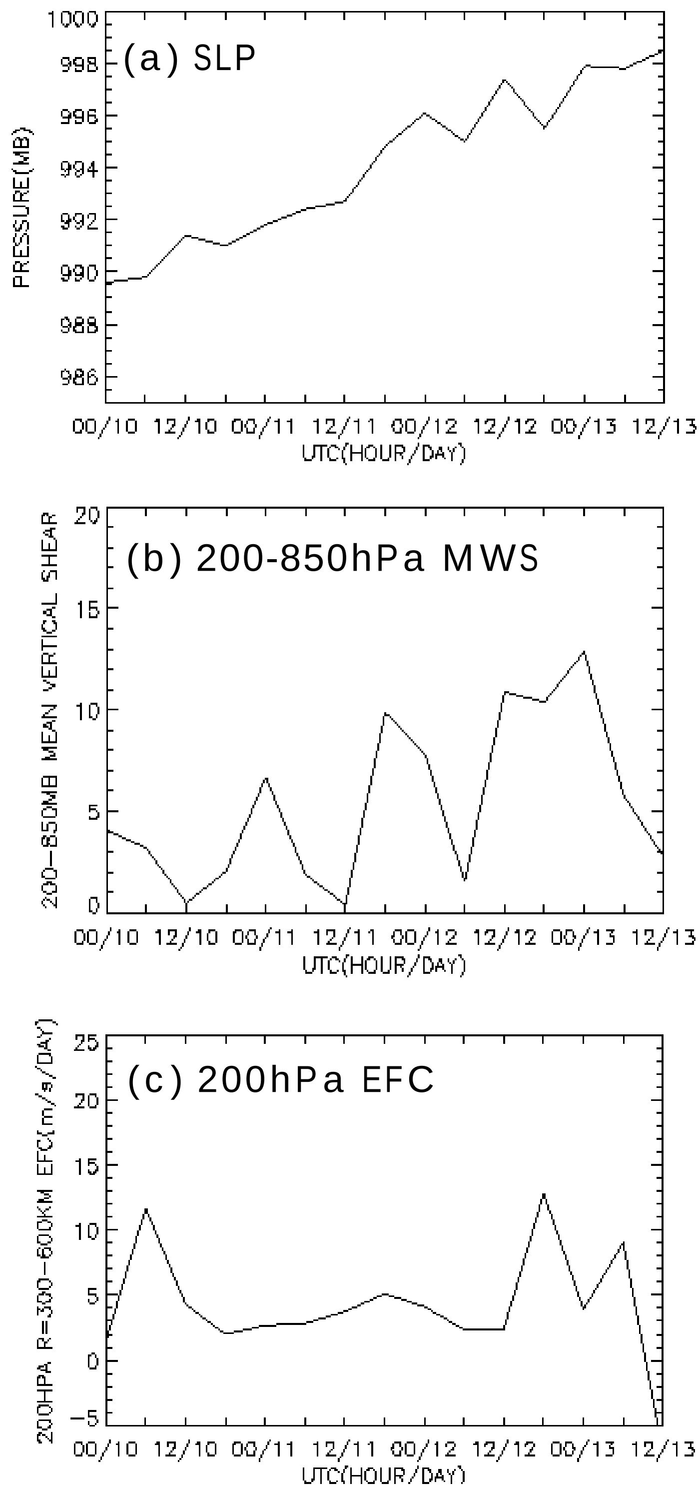

Fig. 5. Time series of (a) sea level pressure, (b) 200-850hPa vertical wind shear, and (c) 200 hPa eddy relative angular momentum flux convergence(EFC) from 0000UTC 10 to 1200UTC 13 July, 2002.

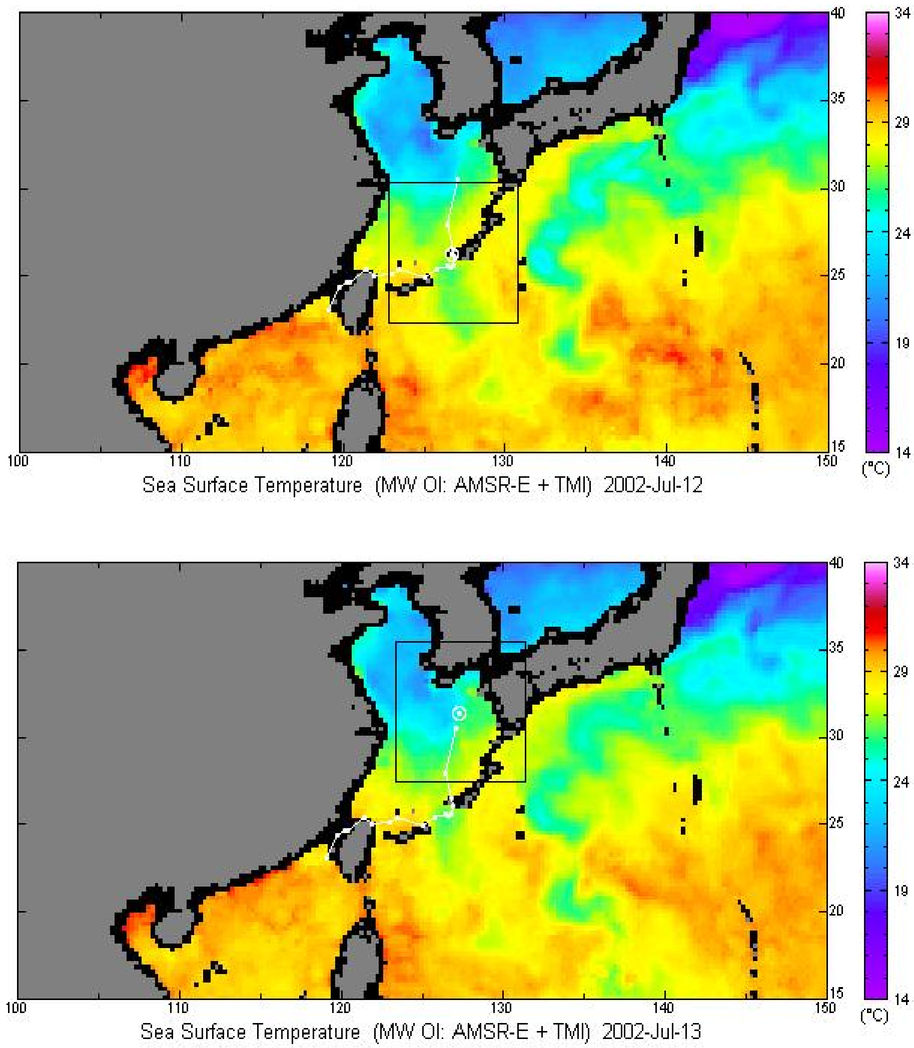

Fig. 6. Daily SST distributions on July 12∼ 13 July, 2002. The white circle in the black box indicates the center of the typhoon.

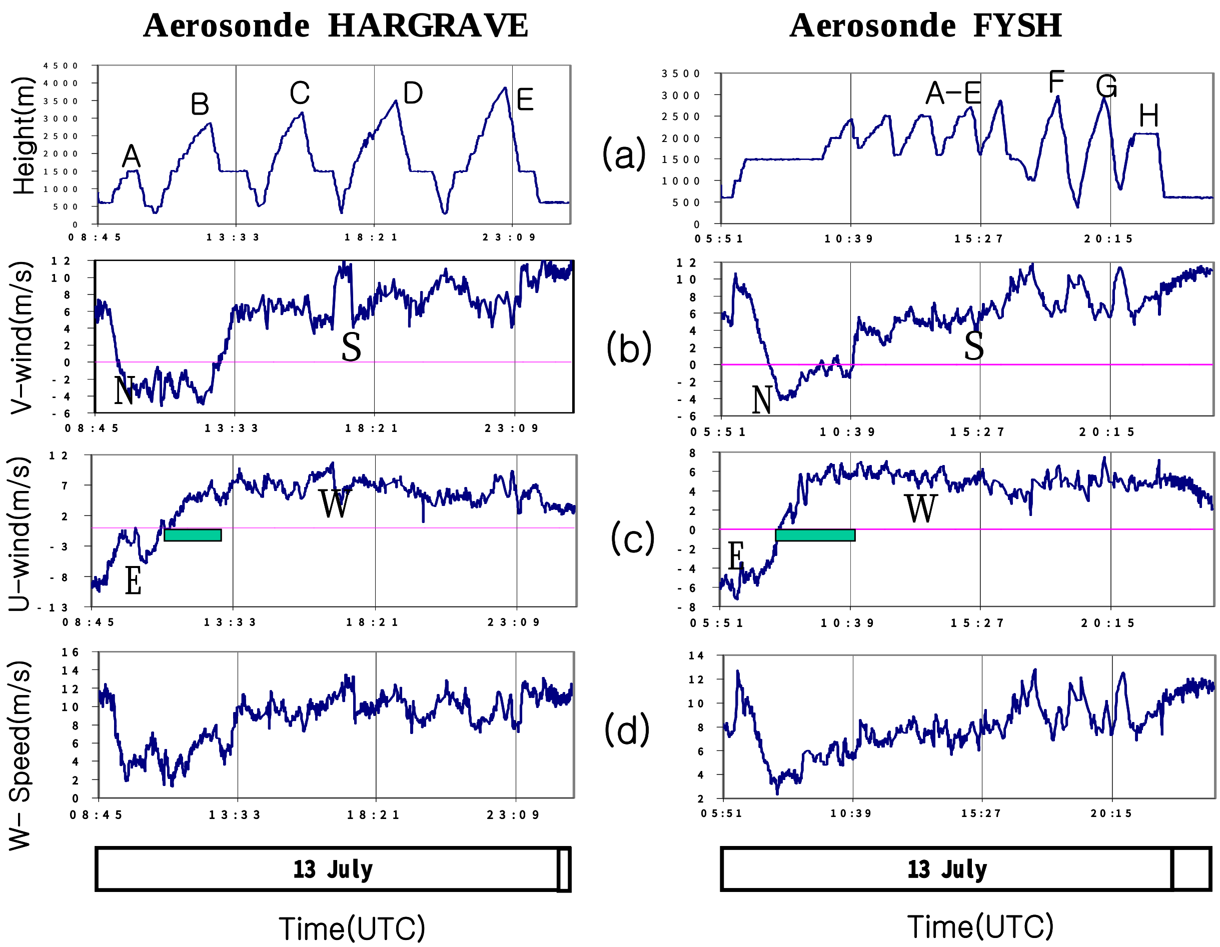

Fig. 7. Time series of (a) altitude, (b) meridional wind, (c) zonal wind and (d) wind speed observed by Aerosondes Hargrave (left panel) and Fysh(right panel). Bold bar indicates the duration of northwesterly.

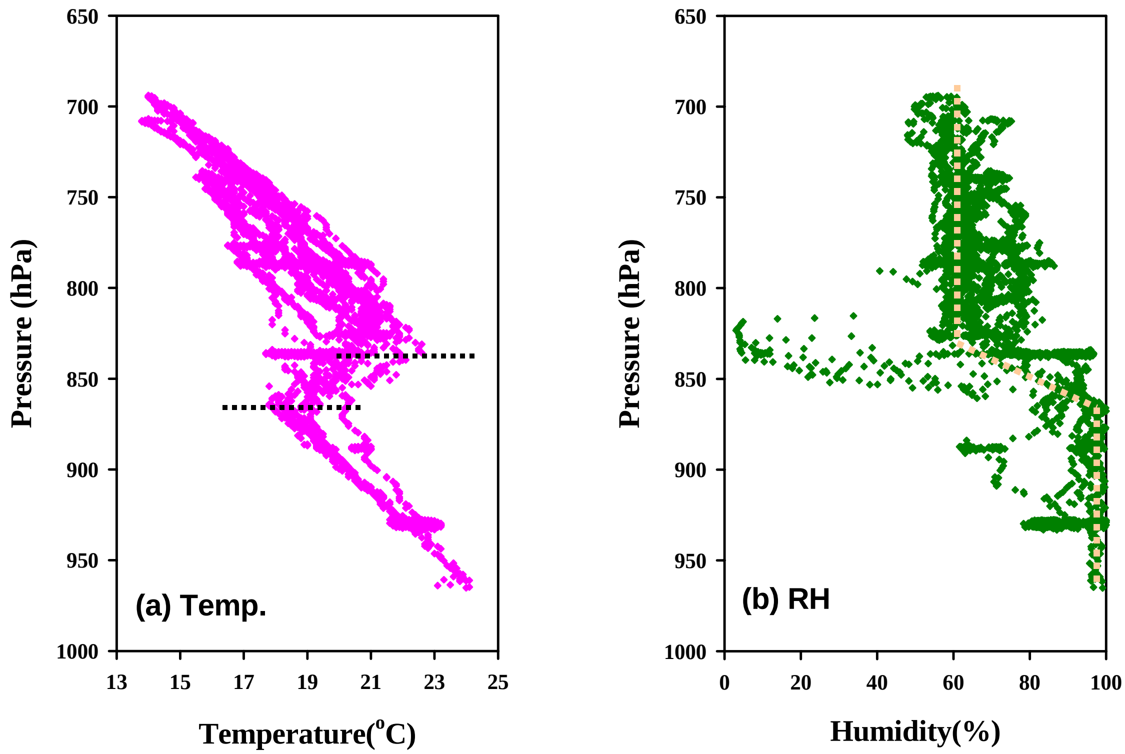

Fig. 8. (a) Temperature and (b) relative humidity from the left wing sensor of Aerosonde FYSH from 0551UTC 13 July to 0002UTC 14 July, 2002. Total number of data is 5,980.

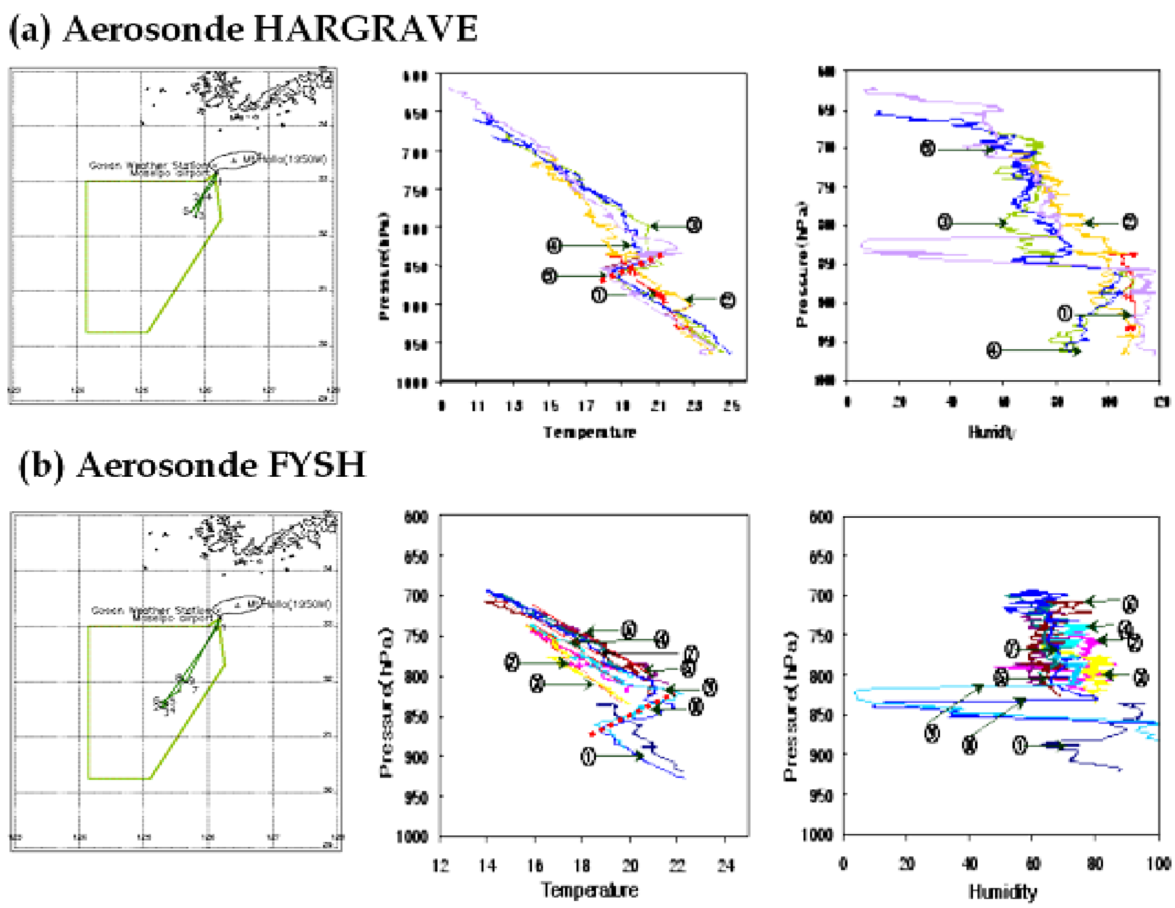

Fig. 9. The locations of Aerosonde's ascendings and temperature and relative humidity profiles observed by its right wing sensor for each ascending of Aerosonde Hargrave and Aerosonde Fysh. Number within parenthesis indicates the serial number of the Aerosonde ascending.